ARTICLE

ACS chemical biology

Genetically Encoded Short Peptide Tags for Orthogonal Protein Labeling by Sfp and AcpS Phosphopantetheinyl Transferases

Zhe Zhou[†,§], Pablo Cironi[‡,§], Alison J. Lin[†,§], Yangqing Xu[‡], Siniša Hrvatin[†], David E. Golan[†], Pamela A. Silver[‡], Christopher T. Walsh[†,*], and Jun Yin[†,¶,*]

[†]Department of Biological Chemistry and Molecular Pharmacology, Harvard Medical School, 240 Longwood Avenue, Boston, Massachusetts 02115 and [‡]Department of Systems Biology, Harvard Medical School, 200 Longwood Avenue, Boston, Massachusetts 02115. [§]These authors contributed equally to this work. [¶]Current address: Department of Chemistry, University of Chicago, 929 E 57th Street, GCIS E505A, Chicago, Illinois, 60637

ABSTRACT Short peptide tags S6 and A1, each 12 residues in length, were identified from a phage-displayed peptide library as efficient substrates for site-specific protein labeling catalyzed by Sfp and AcpS phosphopantetheinyl transferases (PPTases), respectively. S6 and A1 tags were selected for useful levels of orthogonality in reactivities with the PPTases: the catalytic efficiency, k_{cat}/K_m of Sfp-catalyzed S6 serine phosphopantetheinylation was 442-fold greater than that for AcpS. Conversely, the k_{cat}/K_m of AcpS-catalyzed A1 labeling was 30-fold higher than that for Sfp-catalyzed A1 labeling. S6 and A1 peptide tags can be fused to N- or C-termini of proteins for orthogonal labeling of target proteins in cell lysates or on live cell surfaces. The development of the orthogonal S6 and A1 tags represents a significant enhancement of PPTase-catalyzed protein labeling, allowing tandem or iterative covalent attachment of small molecules of diverse structures to the target proteins with high efficiency and specificity.

Recently an efficient method for live cell site-specific protein labeling has been developed using phosphopantetheinyl transferases (PPTases), including Sfp of *Bacillus subtilis* origin and AcpS of *Escherichia coli* origin, to post-translationally modify the peptidyl carrier protein (PCP) or acyl carrier protein (ACP) domains fused to the target proteins on cell surfaces with small-molecule probes of diverse structures (*1, 2*). PCP and ACP domains are small autonomously folding domains, 80–100 residues in size, which can either be embedded or stand alone as key parts of the biosynthetic machinery of nonribosomal peptide synthetases (NRPSs), polyketide synthases (PKSs), and fatty acid synthases (FASs) (*3–6*). In order for those biosynthetic enzymatic assembly lines to be active, every PCP and ACP domain first needs to be post-translationally modified by PPTases for the installation of a 20 Å phosphopantetheinyl (Ppant) prosthetic group through a phosphodiester bond to the hydroxyl group of a conserved serine residue (*7*) (Figure 1, panel a). The Ppant group is derived from coenzyme A (CoASH), the native substrate of PPTases, and functions as a swinging arm, providing successive anchoring points for the attachment of the growing peptide, polyketide, or fatty acyl chains as they elongate down the NRPS, PKS, or FAS enzymatic assembly lines.

In addition to the physiologic substrate CoASH, PPTases such as Sfp and AcpS have been found to display impressive substrate promiscuity toward the small-molecule entities covalently conjugated to CoA through the terminal thiol (*8–11*). This property has been employed for site-specific protein labeling by constructing

*Corresponding authors, christopher_walsh@hms.harvard.edu, junyin@uchicago.edu.

Received for review March 9, 2007 and accepted April 4, 2007.

Published online April 27, 2007

10.1021/cb700054k CCC: $37.00

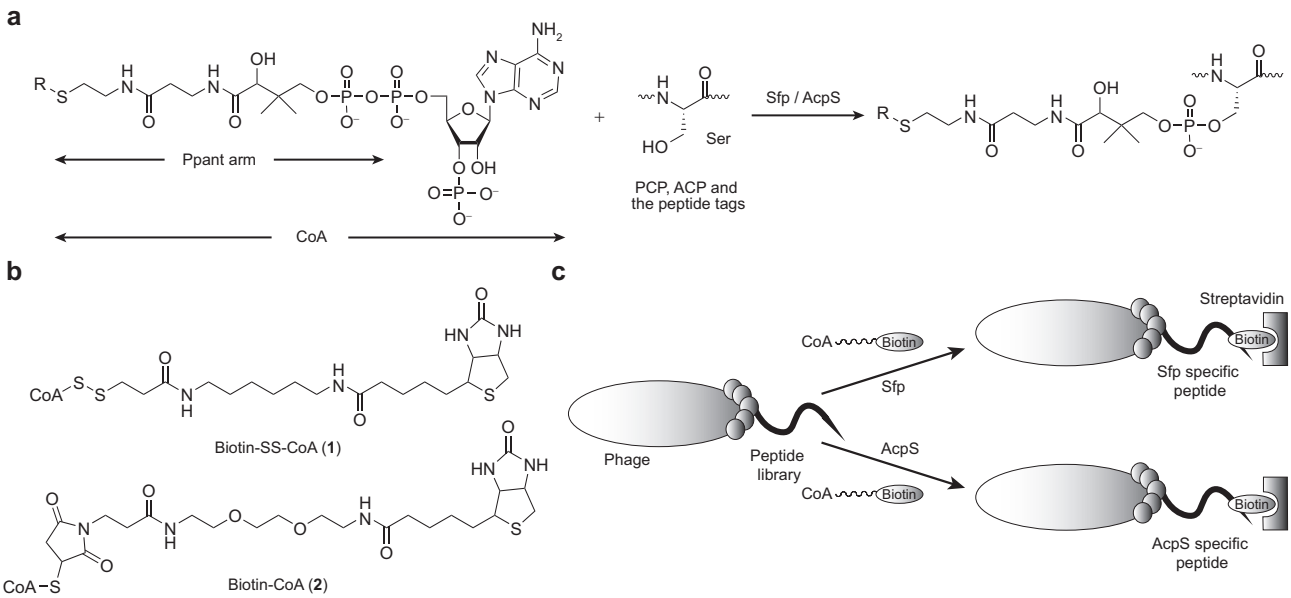

Figure 1. Peptide labeling reaction and the selection scheme of the phage-displayed peptide libraries. a) Sfp- or AcpS-catalyzed PCP, ACP, or peptide labeling reactions using small-molecule-CoA conjugates as the donor of the small-molecule-Ppant group to a specific serine residue in PCP, ACP, or the peptide tags. b) Structures of biotin-SS-CoA (1) and biotin-CoA (2) used in selection and phage ELISA. c) Parallel selection of the peptide substrates of Sfp and AcpS from a phage-displayed peptide library.

fusions of PCP with target proteins and covalently transferring small molecules of diverse structures, including fluorophores, biotin, sugars, peptides, and porphyrin, as phosphopantetheinylated moieties to the PCP tag (*12–15*). Similarly AcpS has been used for post-translational labeling of ACP tags fused to the target protein (*16–18*) (Figure 1, panel a). Applications to date of PPTase-based protein labeling include high-throughput printing of protein microarrays, site-specific attachment of small molecules to phage particles, and live cell imaging of cell surface proteins (*12–18*). Furthermore, Sfp can modify both PCP and ACP domains, whereas AcpS only modifies the ACP domain (*19, 20*). Therefore, it has been demonstrated that cell surface proteins fused to either PCP or ACP tags can be differentially labeled with different fluorophores by the tandem incubation of the cells first with AcpS to label ACP-tagged protein with one type of fluorophore-CoA conjugate followed by Sfp-catalyzed labeling of PCP-tagged protein with another type of fluorophore-CoA conjugate (*18*).

To decrease the size of the 80–100 residue PCP tag to be fused to the target protein, by phage display and then peptide synthesis, we recently identified an 11-residue peptide tag named ybbR as a surrogate substrate of Sfp from a genomic library of *B. subtilis* (*15*). We have also shown that the ybbR tag can be fused to the N- or C-termini of target proteins or, as an alternative, be inserted into a flexible loop of a protein; all of these fusions can then be efficiently labeled with small-molecule probes by Sfp, further improving the versatility of Sfp-catalyzed protein labeling.

Here we report the identification of two new peptide tags, designated S6 and A1, each 12 residues in length, which can serve as efficient substrates of Sfp and AcpS, respectively, on their own and can be used for PPTase-catalyzed site-specific protein labeling. We used parallel phage selections to find orthogonal peptide sequences so that Sfp and AcpS could ultimately be used sequentially for modification of two different targeted proteins in one pot. To this end, S6 and A1 have useful orthogonality, with catalytic efficiencies 442-fold in favor of Sfp for S6 and 30-fold in favor of AcpS for the A1 peptide. We further demonstrated that the S6 tag/Sfp enzyme and the A1 tag/AcpS enzyme could be an orthogonal pair for site-specific protein labeling and imaging of differentially tagged receptor proteins on the surface of the same cell.

RESULTS AND DISCUSSION

Construction of the Phage-Displayed Peptide Library and Selection. We previously found that the minimum requirement for the YbbR peptide to be an efficient substrate of Sfp is the 11-residue DSLEFIASKLA, with the underlined serine being the site of Ppant modification (*15*). We also noted that PCP and ACP domains have a conserved (H/D)S(L/I) motif at the site of Ppant-modified serine (underlined) with the residue preceding the conserved serine a histidine or aspartic acid, and the residue following the serine a leucine or isoleucine (*4*). Consequently, we constructed a peptide library in phagemid pComb3H (*21*) in the form of GDS(L/I) XXXXXXXX (X = any of the 20 protein residues) fused to the N-terminus of M13 phage capsid protein pIII. The final size of the peptide library was $\sim 1 \times 10^9$.

The phage library was selected in parallel in separate tubes by Sfp- and AcpS-catalyzed biotin-Ppant conjugation to the phage-displayed peptides using biotin-SS-CoA (**1**) as the substrate (Figure 1, panels b and c). Subsequently, biotin-conjugated phage particles were bound to streptavidin-coated 96-well plates and after washing cleaved from the solid support by DTT for the next round of selection. After the first round of selection, the library diverged in the subsequent rounds, in that phages selected by Sfp were continued for the next round of Sfp selection and phages selected by AcpS were continued for the next round of AcpS selection (Figure 1, panel c). In parallel to the selection reaction, control reactions were performed excluding the enzymes or biotin-SS-CoA. We found that, round by round, there was a steady increase in the ratio of phage recovery for the selection reactions, including both the enzyme and biotin-SS-CoA (**1**) over the controls (Supplementary Figure 1). The fifth round of selection gave a ratio of 10^4 for the phage recovery from the reaction over the controls, suggesting that the selection was indeed dependent on PPTase-catalyzed biotin modification of the phage-displayed peptides, and the peptide clones enriched from the fifth round could be very efficient substrates of Sfp and AcpS.

After the fifth round of selection, DNA sequencing of the phage clones from either the Sfp-selected or the AcpS-selected pools showed significant sequence convergence of the displayed peptides (Figure 2; Supplementary Figure 2). Supplementary Table 1 lists the designations and the peptide sequences of the most abundant phage clones after the fifth round of selection. Peptide S1 and a closely related sequence S1′ differing by two mutations appeared a total of 6 times among the 30 sequencing samples from the Sfp-selected libraries. Similarly, peptide A1 was counted 8 times among the 40 sequencing samples from the AcpS-selected library. This suggested that S1 and A1 clones started to dominate the final selected pool of peptides, and thus no more selection was carried out after the fifth round.

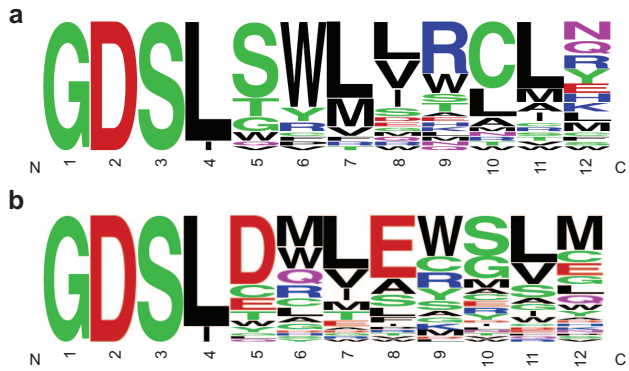

Figure 2. Sequences of the peptides enriched by phage display for Sfp and AcpS modification after five rounds of selection. a) Peptide sequences selected by Sfp modification. b) Peptide sequences selected by AcpS modification. In both panels, the size of the characters denotes the frequency of a specific residue that appeared at the corresponding position among the selected peptides. The first three residues (GDS) were not randomized in the peptide library, with the serine being the site of Ppant attachment. The figures were generated by WebLogo (weblogo.berkeley.edu).

Characterization of the Selected Peptide Clones. Phage enzyme-linked immunosorbent assay (ELISA) showed that phages displaying S1 and A1 peptides were efficiently modified by Sfp or AcpS, respectively, using biotin-CoA (**2**) as the substrate (Figure 1, panel b), as suggested by the strong ELISA signals for the binding of biotinylated phages to the streptavidin plate (Figure 3, rows 1 and 6). In contrast, the level of cross biotin modification of S1-displayed phages with AcpS and A1-displayed phages with Sfp were the same as the background, excluding the enzyme or biotin-CoA in the labeling reaction (Figure 3, rows 2 and 5), suggesting the S1 peptide enriched by Sfp selection was a poor substrate for AcpS and, *vice versa*, the A1 peptide enriched by AcpS selection was a poor substrate for Sfp. Other peptide clones from phage selection, S4, S5, and S9 from the Sfp selection and A2, A3, and A4 from the AcpS selection showed similar results: high level of biotin la-

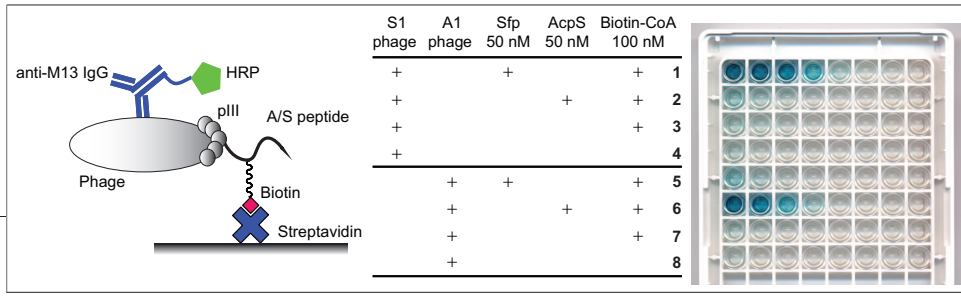

Figure 3. Phage ELISA of the biotin labeling reactions with the phages displaying S1 and A1 peptides. In separate reactions, phages displaying different peptide sequences were labeled with biotin by either Sfp or AcpS using biotin-CoA (2) as the donor of the biotin-Ppant group. Control reactions were also run in parallel with the exclusion of the enzymes or both the enzymes and biotin-CoA (2). After the labeling reaction, the reaction mixtures were added to the streptavidin-coated 96-well plate and diluted across the plate by 5-fold from left to right to allow the binding of biotin-conjugated phage particles to the streptavidin surface. After washing, phages retained in each well were detected using an anti-M13 phage antibody conjugated to horseradish peroxidase (HRP).

beling with the PPTase used for selection and background level of cross-labeling with the other PPTase (Supplementary Figure 3). Thus our selection strategy, that is, starting from the same peptide library that was subsequently diverged by either Sfp- or AcpS-catalyzed biotin labeling through continued rounds of selection, led us to two pools of peptides with preferred substrate specificity with Sfp (S1, S4, S5, and S9) and AcpS (A1, A2, A3, and A4), respectively.

After PPTase-catalyzed modification of selected peptide clones was confirmed by ELISA, 12-residue S1 and A1 peptides were synthesized, and the kinetics of the biotin Ppant transfer reaction from biotin-CoA (**2**) to the peptides catalyzed by Sfp or AcpS were measured (Table 1). Sequence alignment also showed that some peptides selected by Sfp, such as S1′ and S4, differing from S1 by a leucine instead of a valine residue at position 8 (Ppant-modified serine is designated position 3) (Supplementary Table 1). Thus peptide S2 with a valine to leucine mutation at position 8 was synthesized, as well as peptides S3, S6, and S7 with cysteine to leucine and serine mutations at position 10, so that the cysteine residue in the S1 peptide was substituted in order to avoid undesired peptide tag mediated disulfide formation of the target proteins.

The specific activities of the S6 peptide ($k_{cat}/K_m = 0.19\ \mu M^{-1}\ min^{-1}$) and A1 peptide ($k_{cat}/K_m = 0.015\ \mu M^{-1}\ min^{-1}$) were the highest for Sfp- and AcpS-catalyzed peptide modification, respectively (Table 1). The S6 peptide also showed the highest level of specificity for Sfp, with a 442-fold higher k_{cat}/K_m for Sfp-catalyzed peptide labeling than the AcpS-catalyzed reaction. Correspondingly, A1 was a poor substrate for Sfp, with a k_{cat}/K_m of $0.00049\ \mu M^{-1}\ min^{-1}$, 30-fold lower than that of the reaction catalyzed by AcpS. The S6 peptide was also a better peptide tag than the previously identified YbbR tag with a 2-fold lower K_m and >10× higher specificity (k_{cat}/K_m) for Sfp-catalyzed peptide modification than that of AcpS (Table 1). Thus, by phage selection we identified two peptide tags, S6 and A1, which not only are efficient substrates of Sfp and AcpS but also show significant catalytic orthogonality, with S6 a preferred substrate of Sfp and A1 a preferred substrate of AcpS.

Orthogonality of S and A1 Peptide Tags for *in Vitro* Protein Labeling. Peptide tags S1, S2, S6, and A1 were fused to the N-terminus of the enhanced green fluorescence protein (EGFP) and tested for biotin labeling by Sfp or AcpS by ELISA (Figure 4). While the S tags and A

TABLE 1. Kinetic characterization of Sfp- and AcpS-catalyzed peptide labeling reaction by biotin-CoA (2)

		Sfp			AcpS			
Peptide	Sequence	k_{cat} (min^{-1})	K_m (μM)	k_{cat}/K_m ($\mu M^{-1}\ min^{-1}$)	k_{cat} (min^{-1})	K_m (μM)	k_{cat}/K_m ($\mu M^{-1}\ min^{-1}$)	k_{cat}/K_m (Sfp)/ k_{cat}/K_m (AcpS)
YbbR13	DSLEFIASKLA	11	123	0.091	0.81	242	0.0033	28
S1	GDSLSWLVRCLN	4.1	139	0.029	0.042	77.2	0.00054	53
S2	GDSLSWL**L**RCLN	10	120	0.083	0.059	108	0.00055	150
S3	GDSLSWLVR**L**LN	3.1	61.8	0.050	0.034	105	0.00032	156
S6	GDSLSWL**L**R**L**LN	10	51.5	0.19	0.033	76.0	0.00043	442
S7	GDSLSWL**L**R**S**LN	8.4	221	0.038	0.085	254	0.00033	115
		Sfp			AcpS			
Peptide	Sequence	k_{cat} (min^{-1})	K_m (μM)	k_{cat}/K_m ($\mu M^{-1}\ min^{-1}$)	k_{cat} (min^{-1})	K_m (μM)	k_{cat}/K_m ($\mu M^{-1}\ min^{-1}$)	k_{cat}/K_m (AcpS)/ k_{cat}/K_m (Sfp)
A1	GDSLDMLEWSLM	0.26	534	0.00049	1.8	117	0.015	30

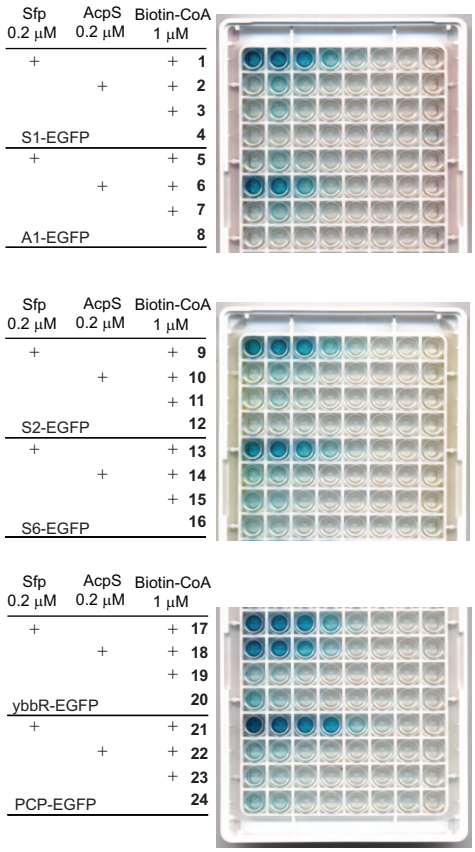

Figure 4. ELISA of N-terminal A1- and S peptide-tagged EGFP labeled with biotin by Sfp- or AcpS-catalyzed protein modification. S- and A1-tagged EGFP were tested for biotin labeling by both Sfp and AcpS using biotin-CoA (2) as the substrate, and the labeling results were compared to biotin labeling of ybbR- or PCP-tagged EGFP. Control reactions were also run with the exclusion of enzymes or both enzymes and biotin-CoA (2). The labeling reaction mixture was loaded on the 96-well streptavidin plate, and 5-fold series dilution was carried out across the wells in the plate. After washing, biotinylated GFP immobilized on the streptavidin surface was detected by mouse anti-GFP antibody and goat anti-mouse antibody-HRP conjugate.

tags showed efficient labeling by Sfp and AcpS, respectively, the ELISA signals for cross-labeling were very low, suggesting the orthogonality of S peptides and the A1 peptide for Sfp- and AcpS-catalyzed protein labeling reactions. S and A1 tags were also fused to the C-terminus of EGFP and the N-terminus of glutathione *S*-transferase or maltose binding protein. All of the fusion proteins demonstrated similar labeling efficiencies, with S-tagged proteins preferentially labeled by Sfp and A1-tagged proteins preferentially labeled by AcpS (data not shown), denoting the portability of the S and A1 tags for the construction of fusions to N- or C-termini of various target proteins. Figure 4 also shows the biotin labeling of N-terminal YbbR- or PCP-tagged EGFP catalyzed by Sfp or AcpS. As expected, PCP-tagged EGFP was preferentially labeled by Sfp, though YbbR-tagged EGFP was significantly labeled by both Sfp and AcpS, suggesting the S tags are more specific substrates for Sfp-catalyzed protein modification than the YbbR tag. S- and A1-tagged EGFP can also be labeled with biotin in the cell lysates by Sfp and AcpS, respectively, as shown by ELISA (data not shown).

To quantify the yield of the protein labeling reaction, S- or A1-tagged EGFP proteins were labeled with biotin by Sfp and AcpS, respectively, followed by the addition of streptavidin-coated agarose beads to pull down the biotin-labeled EGFP (*15*). More than 80% of the S- or A1-tagged EGFP was immobilized on the streptavidin beads after the biotin labeling reaction. In contrast, $<5\%$ of the EGFP was pulled down by streptavidin beads in the cross-labeling reaction using Sfp to label A1-tagged protein or AcpS to label S-tagged protein, denoting the reactive orthogonality of the S6/Sfp and A1/AcpS pairs for protein labeling.

Cell Surface Protein Labeling with the S6 and A1 Peptide Tag. The S6 and A1 tags were fused to epidermal growth factor receptor (EGFR) and transferrin receptor 1 (TfR1), respectively, for the construction of N-terminal S6-EGFR and C-terminal TfR1-A1 fusion proteins, because the N-terminus of EGFR and the C-terminus of TfR1 are exposed on the cell surface, which would expose the tags for protein labeling. HeLa cells were transfected with pUSE containing S6-EGFR and labeled with Texas red-CoA and Sfp. Labeled HeLa cells were treated with Alexa 488-conjugated epidermal growth factor (EGF) ligand that would bind to EGFR. Texas red-labeled S6-EGFR receptor on the cell surface and the binding of Alexa 488-conjugated EGF ligand is demonstrated (Figure 5, panels a–c). The colocalization of the S6-EGFR receptor with the bound EGF ligand suggests that the S6 tag fused to the receptor can be recognized by Sfp for site-specific protein labeling and imaging, and the S6-tagged EGFR can bind the EGF ligand. Similarly, TRVb cells were transfected with pcDNA3.1 containing TfR1-A1. The receptors were labeled with Alexa 488 by AcpS-catalyzed A1 tag modification, and the

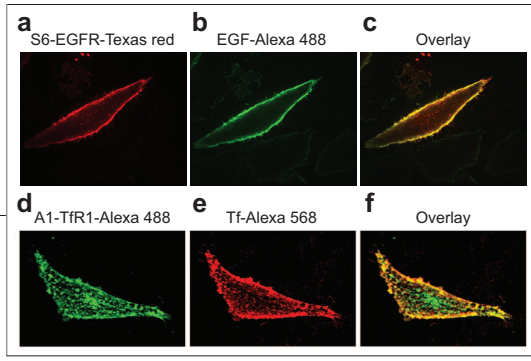

Figure 5. Cell surface labeling of S6- and A1-tagged EGFR and TfR1 receptors with small-molecule fluorophores by Sfp and AcpS. Transfected receptors were labeled in living cells and then fixed for observation. a–c) HeLa cells were transfected with S6-EGFR. Shown are laser confocal images at a single *z* plane of the transfected HeLa cells, with a) Texas red-labeled S6-EGFR in red and b) fluorescently tagged ligand EGF-Alexa 488 in green. c) Overlay of panels a and b. d–f) TRVb cells were transfected with A1-TfR1. Shown are 2D projections of 3D optical stacks of laser confocal images of the transfected TRVb cells, with d) Alexa 488-labeled A1-TfR1 in green and e) fluorescently tagged ligand Tf-Alexa 568 in red. f) Overlay of panels d and e.

cells were incubated with Alexa 568-conjugated transferrin (Tf) ligand (Tf-Alexa568). Figure 5, panels d–f are images of a typical cell showing Alexa 488-labeled TfR1-A1 receptors colocalizing with Tf-Alexa 568 ligand on the cell surface. This suggests that the A1 tag can also be used for cell surface protein labeling without interfering with receptor-ligand binding. The A1 tag was also fused to the N-terminus of EGFR with its C-terminus fused to EGFP. Supplementary Figure 4 illustrates the labeling of A1-EGFR-EGFP with Texas red by AcpS and the colocalization of A1-conjugated Texas red with EGFP, suggesting that the A1 tag can be fused to either the N- or C-terminus of different receptors.

We next demonstrate that two differentially tagged cell surface proteins can be orthogonally labeled with two distinct fluorophores by Sfp- and AcpS-catalyzed S6 and A1 tag modification, respectively. HeLa cells were cotransfected with pUSE-S6-EGFR and pcDNA3.1-TfR1-A1 plasmids and treated sequentially with AcpS in the presence of Alexa 488-CoA to label TfR1-A1 and then with Sfp in the presence of Texas red-CoA to label S6-EGFR. Figure 6 shows images of the sequentially labeled cells, where the distribution of Alexa 488-labeled TfR1-A1 is represented in green (Figure 6, panel a), and the distribution of Texas red-labeled S6-EGFR is represented in red (Figure 6, panel b). Figure 6, panel c shows the overlay of the two labeled receptors, allowing us to simultaneously visualize the distributions of the two receptors on the same cell. This demonstrates that the PPTase orthogonal labeling method with small peptide tags can be applied toward biological studies of intricate relationships between distinct receptors (*22*). Control experiments were performed to further prove the specificity and orthogonality of the labeling with Sfp and AcpS for cell surface receptors. Non-transfected cells were treated with Texas red-CoA in the presence of Sfp or AcpS, and no background labeling was detected (Supplementary Figure 5). Cells transfected with TfR1-A1 or S6-EGFR were also treated with fluorophore-CoA, but in the absence of PPTase there was no enzyme-independent labeling (data not shown). The cross-labeling between the two pairs of tag and PPTase were assessed by non-matching labeling experiments. HeLa cells expressing TfR1 fused with A tag were incubated with Sfp and Texas red-CoA (data not shown), and HeLa cells expressing EGFR fused with S tag were incubated with AcpS and Texas red-CoA (Supplementary Figure 6). In all cases, the resulting fluorescence was extremely low, thus demonstrating that no significant labeling occurs when small A/S tags are used with non-matching PPTases.

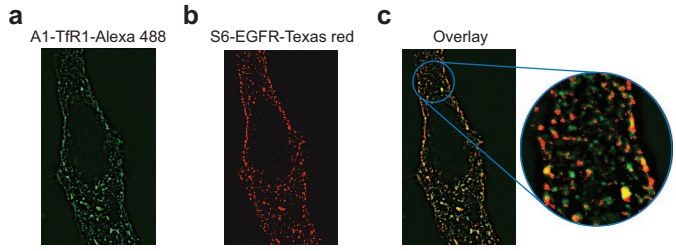

Figure 6. Orthogonal labeling of TfR1 and EGFR receptors on the surface of the same cell. HeLa cells expressing both TfR1-A1 and S6-EGFR were sequentially labeled with Alexa 488 by AcpS-catalyzed A1 modification and with Texas red by Sfp-catalyzed S tag modification. Cells were imaged using laser confocal microscopy for a) TfR1-A1 labeled with Alexa 488 and b) S6-EGFR labeled with Texas red. c) Overlay of panels a and b. The circular picture (panel c) is the enlarged image in the blue circle.

Comparison of the S, A, and ybbR Peptides from the Phage Selection for Sfp and AcpS Modification. The circular dichroism (CD) spectrum of peptide S6 indicates a tendency to adopt an α-helical conformation in 30% trifluoroethanol (TFE), similar to the previously reported Sfp substrate ybbR13 (*15*), while the features for an α-helical conformation in the CD spectrum of the S1 peptide are not as significant (Supplementary Figure 7). These results suggest that S and YbbR peptides may adopt α-helical conformations and mimic the helix II in PCP upon their binding to Sfp. Although the A1 peptide is not structured in 30% TFE (Supplementary Figure 7), it is also reasonable to suspect that the A1 peptide would adopt an α-helical conformation upon its binding to AcpS, similar to the helix II in ACP. In fact, the helix II in

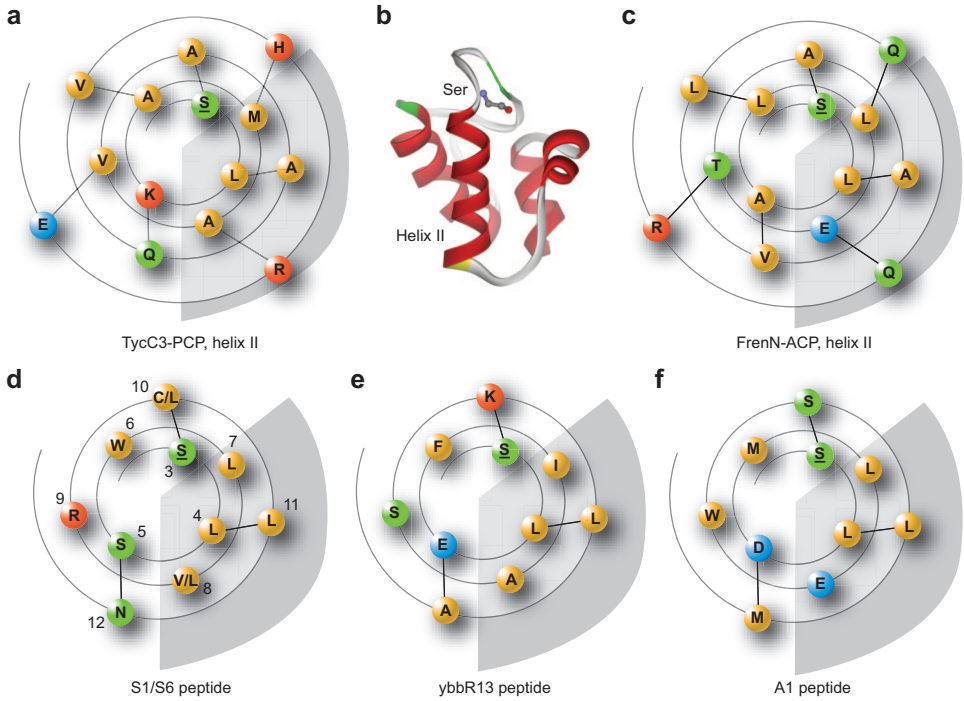

Figure 7. Topology of selected peptides with helix II in the full-length carrier protein. Helical wheel plots of the helix II of a) TycC3-PCP and c) FrenN-ACP, and the phage-selected peptides of d) S6, e) YbbR13, and f) A1 peptides. S6 and TycC3-PCP are preferably modified by Sfp, and A1 and FrenN-ACP are preferably modified by AcpS. YbbR can be modified by both Sfp and AcpS. The NMR structure of TycC3-PCP is also shown in panel b with helix 2 and the Ppant-modified serine residue labeled. Residues on the side of helix 2 exposed to solvent are highlighted by a gray background in the helical wheel plots. The Ppant-modified serine is underlined. Residue color scheme: yellow, nonpolar residues; green, polar uncharged residues; blue, negatively charged residues; red, positively charged residues.

both ACP and PCP proteins has been demonstrated to play an important role for PPTase recognition (*23*).

To compare the topology of the selected peptides with helix II in the full-length carrier protein, the sequences of S6, A1, and YbbR were presented in helical wheel plots and compared with the similar plots representing the helix II of tyrocidine A synthetase (TycC3)-PCP (*24*) and FrenN-ACP (*25*) of which the NMR structures are available (Figure 7). Such a comparison identified significant homology corresponding to the residues occupying the solvent-exposed surface of helix II (Figure 7, residues 4, 7, 8 and 11 with a gray background). For an example, phage selection with Sfp identified peptide S6 with leucine and valine residues occupying positions 4, 7, 8, and 11, clustering on one side of the helix (Figure 7, panel d), quite similar to the solvent-exposed side of helix II in TycC3-PCP with small hydrophobic residues leucine, alanine, and methionine at the same positions (Figure 7, panel a). Phage selection with AcpS-enriched A1 peptide with a negatively charged glutamic acid residue at position 8 with three leucine residues at positions 4, 7, and 11 on the same side of the helix (Figure 7, panel f). This is very similar to the helix II of FrenN-ACP with glutamic acid residue at position 8 and leucine and alanine residues at the corresponding positions on the side of helix exposed to the solvent (Figure 7, panel c). The glutamic acid residue at position 8 in the A1 peptide or in the helix II of ACP provides a negatively charged side chain for interaction with AcpS and is very much different from the small hydrophobic residues at the same position in the S peptides or the full-length PCP modified by Sfp. Therefore, we suspect this glutamic acid residue would play a critical role for the A1 peptide to be specifically recognized by AcpS, and at the same time rejected by Sfp for efficient modification. The YbbR peptide selected from the

B. subtilis library share the same features of the S peptides and the helix II of PCP in terms of the type of the residues positioned on the side of the helix corresponding to the solvent-exposed side of helix II in the carrier proteins (Figure 7, panel e). Thus phage selection of a randomized peptide library has identified peptides preserving the important structure characteristics of helix II of the carrier proteins so that the selected peptides could recapitulate the critical protein–protein interactions between the carrier proteins and the PPTases.

Interestingly we previously found that peptides corresponding to the original sequence of helix II from PCP or ACP domains cannot be modified by the corresponding PPTases (*15, 26*), suggesting the original helix II peptides need to be folded in the context of the full-length carrier proteins in order to be recognized by the PPTases as substrates. The fact that phage selection was able to identify short peptides YbbR, S, and A1 as efficient substrates for PPTase modification denotes the power of molecular evolution for engineering proteins and peptides of unique functions.

Application of S6 and A1 Peptide Tags for Site-Specific Protein Labeling. In the category of site-specific protein labeling carried out by protein post-translational modification enzymes, a number of methods have emerged, including human O^6-alkylguanine-DNA alkyltransferase (*27*), biotin ligase (*28*), transglutaminase (*29*), sortase (*30*), cutinase (*31*), and Sfp or AcpS PPTases for the covalent attachment of the small-molecule probes to the target protein. PPTase-catalyzed protein labeling remains an attractive method with the combined advantage of (i) small size of the peptide tags (12 residues) for the construction of protein fusions with the minimum disturbance to the target protein structure and biological function; and (ii) one-step protein labeling for the direct conjugation of small molecule probes of diverse structures to the tagged target protein; (iii) high efficiency and specificity of the labeling reaction that can be carried out on cell surfaces in culture media or within cell lysates.

Our report on S6 and A1 short peptide tags for orthogonal protein labeling by Sfp and AcpS further increases the versatility of the PPTase-based protein labeling method. We have demonstrated that S6 and A1 can be fused to target proteins at either the N- or C-terminus and can be efficiently labeled with CoA-conjugated small-molecule probes by Sfp and AcpS, respectively. S6 and A1 also show significant orthogonality in reactivity with Sfp and AcpS: the catalytic specificity (k_{cat}/K_m) of Sfp-catalyzed S6 labeling is $>$440-fold higher than AcpS-catalyzed S6 labeling, and *conversely*, the specific specificity (k_{cat}/K_m) of AcpS-catalyzed A1 labeling is $>$30-fold higher than Sfp-catalyzed A1 labeling (Table 1). Correspondingly, we have shown that EGFP proteins fused with the S6 tag or the A1 tag are efficiently labeled with biotinyl-Ppant by Sfp or AcpS, respectively (Figure 4). The cross-labeling of S- tagged EGFP by AcpS and A1-tagged EGFP by Sfp are at least 25-fold lower than the labeling of the S6 and A1 tagged proteins by the cognate PPTase of each tag, Sfp for the S6 tag and AcpS for the A1 tag. This opens the door for using the S6/Sfp and A1/AcpS pair for the sequential labeling of two proteins with different small-molecule probes with very little cross-labeling.

Previously it has been reported that ACP- or PCP-tagged receptors expressed on the surface of different yeast cells can be labeled with different fluorophores by sequential carrier protein modification catalyzed by AcpS and Sfp (*18*). Here we show that, on the surface of the same cell, S6- or A1-tagged EGFR and TfR1 receptors can be labeled with different fluorophores by sequential short peptide tag modification catalyzed by the same pair of enzymes, AcpS and Sfp (Figure 6). Thus, our results demonstrate not only that the PPTase-catalyzed sequential protein labeling reaction can be used for orthogonal labeling and simultaneous imaging of two distinct proteins on the surface of the same cell, but also that the orthogonal labeling reaction can be accomplished by tagging the target proteins with 12-residue short peptide tags A1 and S6, much smaller than the full-length ACP or PCP proteins of at least 75 residues in size.

As a result of the multiple negative charges on the ATP moiety of CoASH, CoA-conjugated small-molecule probes are not membrane-permeable, and thus Sfp- or AcpS-catalyzed protein labeling is currently limited to labeling proteins in cell lysates or on the cell surface. One advantage of the inability of the CoA-fluorescent dye conjugate to penetrate the membrane is that the intracellular background fluorescence is very low after extracellular labeling of the cell with the conjugate. This feature allows high-contrast imaging of the intracellular trafficking of internalized cell surface receptors.

In summary, we have developed two 12-residue short peptide tags S6 and A1 with orthogonal sub-

strate specificities for the site-specific protein post-translational labeling reaction catalyzed by PPTases Sfp and AcpS. The small size of the S6 and A1 tags compared to the full-length PCP and ACP domains (80–100 residues), the versatility of those tags for fusion to target proteins at N- or C-termini, the structural diversities of the small-molecule probes for Sfp- and AcpS-catalyzed peptide modification, and the high efficiency and specificity of Sfp and AcpS for the S6 and A1 tags provide a powerful protein labeling method that would allow specific orthogonal labeling of different target proteins on cell surfaces or in cell lysates.

METHODS

Cell Surface Labeling of TfR1-A1. TRVb cells (a kind gift of Timothy E. McGraw, Weill Medical College, Cornell University) expressing TfR1-A1 (transfection protocols available in Supporting Information) were incubated with 1.98 μM AcpS, 1 μM CoA-Alexa Fluor 488, 10 mM $MgCl_2$, 50 mM HEPES, pH 7.5 in 200 μL of serum-free media for 30 min at 37 °C under 5% CO_2. Cells were washed five times with PBS, incubated with 10 μg mL^{-1} Alexa Fluor 568-conjugated Tf, and then washed five times with PBS. Finally, cells were fixed at 4 °C for 10 min using a 3.7% formaldehyde solution in PBS and mounted with mounting medium AEC (Immunotech) for optical microscopy studies. We have conducted experiments to optimize the labeling time for single color labeling and have found that 15–40 min of incubation with the solution containing the enzyme and the fluorophores was the most favorable for imaging experiments (data not shown).

Cell Surface Labeling of S6-EGFR. HeLa cells expressing S6-EGFR (transfection protocols available in Supporting Information) were incubated with 1.98 μM Sfp, 1 μM CoA-Texas red, 10 mM $MgCl_2$, 50 mM HEPES, pH 7.5 in 200 μL of serum-free (not required) media for 20 min at 37 °C under 5% CO_2. Cells were washed five times with PBS, incubated with 5 μg mL^{-1} Alexa Fluor 488-conjugated EGF (Molecular Probes Inc.) for 5 min, and then washed five times with PBS. Finally, cells were fixed and mounted for optical microscopy studies.

Cell Surface Labeling of A1-TfR1 and S6-EGFR Expressed in HeLa Cells. TfR1-A1 was labeled first by incubating the cells with 1.98 μM AcpS, 1 μM CoA-Alexa Fluor 488, 10 mM $MgCl_2$, 50 mM HEPES, pH 7.5 in 200 μL of serum-free media (not required) for 30 min at 37 °C under 5% CO_2. Labeled cells were washed five times with PBS and then incubated with 1.98 μM Sfp, 1 μM CoA-Texas red, 10 mM $MgCl_2$, 50 mM HEPES, pH 7.5 in 200 μL of serum-free media for 20 min at 37 °C under 5% CO_2. Cells were washed five times with PBS then fixed and mounted with mounting medium for optical microscopy studies.

Images were acquired with a confocal microscopy using a Nikon TE2000U inverted microscope in conjunction with a PerkinElmer Ultraview spinning disk confocal system or in a Nikon Eclipse TE2000-E inverted epifluorescence microscope equipped with a Hamamatsu Orca ER Cooled-CCD camera. Images were acquired using a 40×, 60×, or 100× differential interference contrast oil immersion objective lens and analyzed using MetaMorph software from Universal Imaging, Inc.

Acknowledgment: This work was supported by grants HL32854 and HL70819 to D.E.G. and GM20011 to C.T.W. from the National Institutes of Health. P.C. was supported by a Fulbright-M.E.C. (Spain) postdoctoral fellowship. J.Y. was supported by a startup find from the University of Chicago. Confocal microscopy was performed in the Nikon Imaging Center at Harvard Medical School.

Supporting Information Available: This material is available free of charge *via* the Internet.

REFERENCES

1. Johnsson, N., George, N., and Johnsson, K. (2005) Protein chemistry on the surface of living cells, *ChemBioChem 6*, 47–52.
2. Yin, J., Lin, A. J., Golan, D. E., and Walsh, C. T. (2006) Site-specific protein labeling by Sfp phosphopantetheinyl transferase, *Nat. Protoc. 1*, 280–285.
3. Cane, D. E., Walsh, C. T., and Khosla, C. (1998) Harnessing the biosynthetic code: combinations, permutations, and mutations, *Science 282*, 63–68.
4. Marahiel, M. A., Stachelhaus, T., and Mootz, H. D. (1997) Modular peptide synthetases involved in nonribosomal peptide synthesis, *Chem. Rev. 97*, 2651–2674.
5. Staunton, J., and Weissman, K. J. (2001) Polyketide biosynthesis: a millennium review, *Nat. Prod. Rep. 18*, 380–416.
6. Wakil, S. J., Stoops, J. K., and Joshi, V. C. (1983) Fatty acid synthesis and its regulation, *Annu. Rev. Biochem. 52*, 537–579.
7. Walsh, C. T., Gehring, A. M., Weinreb, P. H., Quadri, L. E., and Flugel, R. S. (1997) Post-translational modification of polyketide and nonribosomal peptide synthases, *Curr. Opin. Chem. Biol. 1*, 309–315.
8. Belshaw, P. J., Walsh, C. T., and Stachelhaus, T. (1999) Aminoacyl-CoAs as probes of condensation domain selectivity in nonribosomal peptide synthesis, *Science 284*, 486–489.
9. Gehring, A. M., Lambalot, R. H., Vogel, K. W., Drueckhammer, D. G., and Walsh, C. T. (1997) Ability of *Streptomyces* spp. acyl carrier proteins and coenzyme A analogs to serve as substrates in vitro for *E. coli* holo-ACP synthase, *Chem. Biol. 4*, 17–24.
10. La Clair, J. J., Foley, T. L., Schegg, T. R., Regan, C. M., and Burkart, M. D. (2004) Manipulation of carrier proteins in antibiotic biosynthesis, *Chem. Biol. 11*, 195–201.
11. Sieber, S. A., Walsh, C. T., and Marahiel, M. A. (2003) Loading peptidyl-coenzyme A onto peptidyl carrier proteins: a novel approach in characterizing macrocyclization by thioesterase domains, *J. Am. Chem. Soc. 125*, 10862–10866.
12. Yin, J., Liu, F., Li, X., and Walsh, C. T. (2004) Labeling proteins with small molecules by site-specific posttranlational modification, *J. Am. Chem. Soc. 126*, 7754–7755.
13. Yin, J., Lin, A. J., Buckett, P. D., Wessling-Resnick, M., Golan, D. E., and Walsh, C. T. (2005) Single-cell FRET imaging of transferrin receptor trafficking dynamics by Sfp catalyzed site specific protein labeling, *Chem. Biol. 12*, 999–1006.
14. Yin, J., Liu, F., Schinke, M., Daly, C., and Walsh, C. T. (2004) Phagemid encoded small molecules for high throughput screening of chemical libraries, *J. Am. Chem. Soc. 126*, 13570–13571.
15. Yin, J., Straight, P. D., McLaughlin, S. M., Zhou, Z., Lin, A. J., Golan, D. E., Kelleher, N. L., Kolter, R., and Walsh, C. T. (2005) Genetically encoded short peptide tag for versatile protein labeling by Sfp phosphopantetheinyl transferase, *Proc. Natl. Acad. Sci. U.S.A. 102*, 15815–15820.

16. George, N., Pick, H., Vogel, H., Johnsson, N., and Johnsson, K. (2004) Specific labeling of cell surface proteins with chemically diverse compounds, *J. Am. Chem. Soc. 126*, 8896–8897.
17. Meyer, B. H., Segura, J. M., Martinez, K. L., Hovius, R., George, N., Johnsson, K., and Vogel, H. (2006) FRET imaging reveals that functional neurokinin-1 receptors are monomeric and reside in membrane microdomains of live cells, *Proc. Natl. Acad. Sci. U.S.A. 103*, 2138–2143.
18. Vivero-Pol, L., George, N., Krumm, H., Johnsson, K., and Johnsson, N. (2005) Multicolor imaging of cell surface proteins, *J. Am. Chem. Soc. 127*, 12770–12771.
19. Flugel, R. S., Hwangbo, Y., Lambalot, R. H., Cronan, J. E., Jr., and Walsh, C. T. (2000) Holo-(acyl carrier protein) synthase and phosphopantetheinyl transfer in *Escherichia coli*, *J. Biol. Chem. 275*, 959–968.
20. Lambalot, R. H., Gehring, A. M., Flugel, R. S., Zuber, P., LaCelle, M., Marahiel, M. A., Reid, R., Khosla, C., and Walsh, C. T. (1996) A new enzyme superfamily—the phosphopantetheinyl transferases, *Chem. Biol. 3*, 923–936.
21. Barbas, C. F., 3rd, Kang, A. S., Lerner, R. A., and Benkovic, S. J. (1991) Assembly of combinatorial antibody libraries on phage surfaces: the gene III site, *Proc. Natl. Acad. Sci. U.S.A. 88*, 7978–7982.
22. Johannessen, L. E., Pedersen, N. M., Pedersen, K. W., Madshus, I. H., and Stang, E. (2006) Activation of the epidermal growth factor (EGF) receptor induces formation of EGF receptor- and Grb2-containing clathrin-coated pits, *Mol. Cell. Biol. 26*, 389–401.
23. Mofid, M. R., Finking, R., and Marahiel, M. A. (2002) Recognition of hybrid peptidyl carrier proteins/acyl carrier proteins in nonribosomal peptide synthetase modules by the 4′-phosphopantetheinyl transferases AcpS and Sfp, *J. Biol. Chem. 277*, 17023–17031.
24. Weber, T., Baumgartner, R., Renner, C., Marahiel, M. A., and Holak, T. A. (2000) Solution structure of PCP, a prototype for the peptidyl carrier domains of modular peptide synthetases, *Structure 8*, 407–418.
25. Li, Q., Khosla, C., Puglisi, J. D., and Liu, C. W. (2003) Solution structure and backbone dynamics of the holo form of the frenolicin acyl carrier protein, *Biochemistry 42*, 4648–4657.
26. Quadri, L. E., Weinreb, P. H., Lei, M., Nakano, M. M., Zuber, P., and Walsh, C. T. (1998) Characterization of Sfp, a Bacillus subtilis phosphopantetheinyl transferase for peptidyl carrier protein domains in peptide synthetases, *Biochemistry 37*, 1585–1595.
27. Keppler, A., Gendreizig, S., Gronemeyer, T., Pick, H., Vogel, H., and Johnsson, K. (2003) A general method for the covalent labeling of fusion proteins with small molecules in vivo, *Nat. Biotechnol. 21*, 86–89.
28. Chen, I., Howarth, M., Lin, W., and Ting, A. Y. (2005) Site-specific labeling of cell surface proteins with biophysical probes using biotin ligase, *Nat. Methods 2*, 99–104.
29. Lin, C. W., and Ting, A. Y. (2006) Transglutaminase-catalyzed site-specific conjugation of small-molecule probes to proteins in vitro and on the surface of living cells, *J. Am. Chem. Soc. 128*, 4542–4543.
30. Mao, H., Hart, S. A., Schink, A., and Pollok, B. A. (2004) Sortase-mediated protein ligation: a new method for protein engineering, *J. Am. Chem. Soc. 126*, 2670–2671.
31. Hodneland, C. D., Lee, Y. S., Min, D. H., and Mrksich, M. (2002) Selective immobilization of proteins to self-assembled monolayers presenting active site-directed capture ligands, *Proc. Natl. Acad. Sci. U.S.A. 99*, 5048–5052.
32. Vivero-Pol, L., George, N., Krumm, H., Johnsson, K., and Johnsson, N. (2005) Multicolor imaging of cell surface proteins, *J. Am. Chem. Soc. 127*, 12770–12771.